British Journal of Pharmacology

DOI:10.1111/j.1476-5381.2012.01882.x
www.brjpharmacol.org

RESEARCH PAPER

The omega-3 polyunsaturated fatty acid eicosapentaenoic acid inhibits mouse MC-26 colorectal cancer cell liver metastasis via inhibition of PGE_2-dependent cell motility

Correspondence
MA Hull, Section of Molecular Gastroenterology, Leeds Institute of Molecular Medicine, Wellcome Trust Brenner Building, St James's University Hospital, Leeds LS9 7TF, UK. E-mail: m.a.hull@leeds.ac.uk

*These authors contributed equally to the work.

Keywords
COX; eicosapentaenoic acid; EP4 receptor; omega-3 polyunsaturated fatty acid; PG

Received
18 October 2011
Revised
22 December 2011
Accepted
18 January 2012

G Hawcroft[1]*, M Volpato[1]*, G Marston[1], N Ingram[1], SL Perry[1], AJ Cockbain[1], AD Race[2], A Munarini[3], A Belluzzi[3], PM Loadman[2], PL Coletta[1] and MA Hull[1]

[1]*Section of Molecular Gastroenterology, Leeds Institute of Molecular Medicine, Wellcome Trust Brenner Building, St James's University Hospital, Leeds, UK,* [2]*Yorkshire Experimental Cancer Medicine Centre, Institute of Cancer Therapeutics, University of Bradford, Bradford, UK, and* [3]*Department of Gastroenterology, Sant'Orsola Malpighi Hospital, University of Bologna, Bologna, Italy*

BACKGROUND AND PURPOSE

The omega-3 polyunsaturated fatty acid (PUFA) eicosapentaenoic acid (EPA) has antineoplastic activity at early stages of colorectal carcinogenesis, relevant to chemoprevention of colorectal cancer (CRC). We tested the hypothesis that EPA also has anti-CRC activity at later stages of colorectal carcinogenesis, relevant to treatment of metastatic CRC, via modulation of E-type PG synthesis.

EXPERIMENTAL APPROACH

A *BALB/c* mouse model, in which intrasplenic injection of syngeneic MC-26 mouse CRC cells leads to development of liver metastases, was used. Dietary EPA was administered in the free fatty acid (FFA) form for 2 weeks before and after ultrasound-guided intrasplenic injection of 1×10^6 MC-26 cells ($n = 16$ each group).

KEY RESULTS

Treatment with 5% (w w^{-1}) EPA-FFA was associated with a reduced MC-26 mouse CRC cell liver tumour burden compared with control animals (median liver weight 1.03 g vs. 1.62 g; $P < 0.034$). Administration of 5% EPA-FFA was also linked to a significant increase in tumour EPA incorporation and lower intratumoural PGE_2 levels (with concomitant increased production of PGE_3). Liver tumours from 5% EPA-FFA- treated mice demonstrated decreased 5-bromo-2-deoxyuridine-positive CRC cell proliferation and reduced phosphorylated ERK 1/2 expression at the invasive edge of tumours. A concentration-dependent reduction in MC-26 CRC cell Transwell® migration following EPA-FFA treatment (50–200 μM) *in vitro* was rescued by exogenous PGE_2 (10 μM) and PGE_1-alcohol (1 μM).

CONCLUSIONS AND IMPLICATIONS

EPA-FFA inhibits MC-26 CRC cell liver metastasis. EPA incorporation is associated with a 'PGE_2 to PGE_3 switch' in liver tumours. Inhibition of PGE_2-EP_4 receptor-dependent CRC cell motility probably contributes to the antineoplastic activity of EPA.

Abbreviations

AA, arachidonic acid; BrdU, 5-bromo-2-deoxyuridine; CRC, colorectal cancer; DHA, docosahexaenoic acid; DMSO, dimethyl sulfoxide; EPA, eicosapentaenoic acid; FAP, familial adenomatous polyposis; FFA, free fatty acid; PI, proliferation index; PUFA, polyunsaturated fatty acid; RCT, randomized controlled trial; TBS, Tris-buffered saline; TTBS, Tween-Tris-buffered saline

Introduction

There is substantial evidence that the omega (ω)-3 polyunsaturated fatty acid (PUFA) eicosapentaenoic acid (EPA) has anti-colorectal cancer (CRC) activity, ranging from *in vitro* studies of the effect of EPA on human CRC cells, to efficacy in rodent models of colorectal carcinogenesis, and human epidemiological observations of the association between dietary ω-3 PUFA intake and decreased CRC risk (Cockbain *et al.*, 2012).

Research has previously focused on the role of EPA for prevention of CRC. EPA has antineoplastic activity in rodent chemical carcinogenesis models (Deschner *et al.*, 1990) and the $Apc^{Min/+}$ mouse model of familial adenomatous polyposis (FAP; Petrik *et al.*, 2000; Fini *et al.*, 2010), as well as chemopreventative efficacy in FAP patients (West *et al.*, 2010).

However, there is also evidence that EPA may have utility for *treatment* of established CRC. Two independent studies have demonstrated efficacy of EPA alone, or in combination with docosahexaenoic acid (DHA), in reducing the number and size of metastatic CRC liver tumours in rodents (Iwamoto *et al.*, 1998; Gutt *et al.*, 2007). However, another study, using a similar rat model of CRC liver metastasis, reported an actual increase in tumour burden associated with administration of a high-dose EPA/DHA mix (Griffini *et al.*, 1998).

There is an unmet clinical need for safe and well-tolerated therapy for advanced, inoperable CRC, either alone or in combination with other chemotherapeutics. Therefore, we investigated the effect of EPA on growth of MC-26 CRC cell liver tumours in *BALB/c* mice. Our recent randomized controlled trial (RCT) in FAP patients used the free fatty acid (FFA) form of EPA (West *et al.*, 2010) and EPA-FFA has been used successfully in the $Apc^{Min/+}$ mouse model of FAP (Fini *et al.*, 2010). The FFA form of EPA is more efficiently absorbed in the small intestine than ethyl ester or triglyceride conjugates (Lawson and Hughes, 1988), providing the rationale for testing orally administered EPA-FFA in our mouse model of CRC liver metastasis.

The mechanism(s) underlying the antineoplastic activity of EPA remains unclear (Chapkin *et al.*, 2007; Cockbain *et al.*, 2012). The critical role of pro-tumourigenic COX-PG signalling in colorectal carcinogenesis and tumour growth is established (Wang and DuBois, 2010). We, and others, have reported that EPA inhibits COX-2-dependent PGE_2 synthesis, with concomitant production of the equivalent 'three-series' PG, PGE_3 in human cancer cells *in vitro* (Yang *et al.*, 2004; Hawcroft *et al.*, 2010) and colorectal mucosa *in vivo* (Vanamala *et al.*, 2008). However, the presence of an 'E_2-to-E_3' switch has never been confirmed in tumour tissue *in vivo*. Therefore, we measured ω-3 PUFA incorporation and levels of E-type PGs in control and EPA-FFA-treated MC-26 CRC cell tumours.

Herein, we report that EPA-FFA treatment inhibits growth of MC-26 mouse CRC liver tumours. Reduced liver tumour burden was associated with tumour EPA incorporation, reduced ω-6 PUFA arachidonic acid (AA) content and lower intra-tumoural PGE_2 levels (with concomitant production of PGE_3). Further mechanistic studies determined that EPA-FFA treatment was associated with decreased CRC cell proliferation and reduced ERK signalling at the invasive edge of tumours. Reduced MC-26 CRC cell motility associated with EPA-FFA treatment *in vitro* was rescued by exogenous PGE_2 confirming that negative regulation of PGE_2-dependent CRC cell invasion contributes to the antineoplastic activity of EPA.

Methods

Drug and receptor nomenclature conforms to the *British Journal of Pharmacology* Guide to Receptors and Channels, 5th Edition (2011) throughout (Alexander *et al.*, 2011).

Mouse MC-26 CRC cells

Mouse colon 26 (MC-26) cells were obtained from the National Cancer Institute, Frederick, MD, USA. Cells were cultured in RPMI 1640 medium containing Glutamax® supplemented with 10% (v v^{-1}) heat-inactivated FBS (all Invitrogen, Paisley, UK), at 37°C in a humidified atmosphere containing 5% CO_2. Cells were routinely sub-cultured using 0.25% (w v^{-1}) trypsin (Invitrogen). Viable cells were counted using a haemocytometer in the presence of 0.04% (v v^{-1}) trypan blue (Sigma-Aldrich, Poole, UK).

BALB/c mouse model of CRC liver metastasis

BALB/c AnN mice were obtained from Charles River UK Ltd. (Margate, UK) and were housed in a specific pathogen-free environment. All experiments were undertaken with UK Home Office approval. Female 8 to 11 week-old *BALB/c* mice were fed one of three isocaloric test diets (n = 16 per group), based on a modified AIN-93G diet base, *ad libitum* for 14 days, in which 7% soybean oil was replaced by corn oil (Supporting Information Table S1). The diets contained either; (i) no EPA-FFA; (ii) 2.5% (w w^{-1}) EPA-FFA; or (iii) 5% (w w^{-1}) EPA-FFA, replacing an equivalent amount of corn oil (Supporting Information Table S1). EPA-FFA was provided by SLA Pharma AG (Watford, UK). Fresh irradiated diet was manufactured by IPS (London, UK) every 8 days and delivered within 24 h in irradiated, vacuum-packed 100 g foil bags in order to minimize oxidation. Uneaten diet was removed, weighed and replaced every day with fresh diet from a previously unopened foil bag.

On day 15, 1×10^6 viable MC-26 mouse CRC cells were suspended in 100 µL sterile PBS and were introduced into the spleen by percutaneous injection with a sterile 27G needle guided by high-frequency, ultrasound imaging (Vevo770, VisualSonics Inc., Toronto, ON, Canada) under 3% (v v^{-1}) isofluorane anaesthesia. Animals continued on the same diet and were weighed daily for a further 14 days until killed by CO_2 asphyxiation, except for 4 mice in the 5% EPA-FFA group, which were killed between days 10–13 post-injection due to ill-health.

One hour before killing, animals received an i.p. injection of 0.75 $mg \cdot kg^{-1}$ 5-bromo-2-deoxyuridine (BrdU; GE Healthcare, Amersham, UK). Immediately after killing, total body, liver and spleen weights were measured by a person blind to the treatment allocation of each mouse. Tumour, normal liver and spleen tissue was fixed in 4% (w v^{-1}) paraformaldehyde in PBS overnight, before being embedded in paraffin, or was snap-frozen in liquid N_2, either un-mounted or mounted in OCT embedding compound (FLUKA Analytical, Exeter, UK).

Measurement of tissue PUFA content

Total PUFA content of tumour tissue and adjacent normal liver was measured by GC-MS as described previously (Hillier

et al., 1991). Data are expressed as the relative % total PUFA content of each PUFA.

Measurement of PGE_2 and PGE_3 levels

Frozen tissue was homogenized in approximately 10 parts 0.9% (w v^{-1}) saline and then centrifuged at 10 000× *g* for 5 min. PGE_2 and PGE_3 levels were measured by LC-MS/MS as described previously (Hawcroft *et al.*, 2010).

Measurement of tumour proliferation index

Sections (4 μm thick) were dewaxed in xylene and rehydrated with alcohol followed by washing in water for 5 min. Sections underwent antigen retrieval by microwave heating in 10 mM citrate buffer (pH 6.0) at 100°C for 10 min. Sections were then rinsed in water before endogenous peroxidase activity was blocked with 0.3% (v v^{-1}) H_2O_2 (Fisher Scientific UK Ltd, Loughborough, UK) in 100% methanol for 10 min at room temperature. Slides were rinsed in Tris-buffered saline (TBS; 50 mM Tris and 0.15 M NaCl, pH 7.4) at room temperature and then blocked with casein (Vector Laboratories UK, Peterborough, UK) in TBS for 30 min. Sections were incubated for 20 min with monoclonal anti-BrdU antibody (clone BU-1) as per manufacturer's instructions (GE Healthcare) in Sequenza® slide racks (Thermo Scientific, Basingstoke, UK). After being washed in Tween-TBS (TTBS; 50 mM Tris and 0.15 M NaCl, pH 7.4, 0.25% Tween 20) twice for 3 min and then TBS once for 3 min at room temperature, sections were visualized using the anti-mouse Envision™ system (DakoCytomation Ltd, Ely, UK). Sections were counterstained in Mayer's haematoxylin for 1 min, dehydrated using alcohol and xylene and mounted using DPX (FLUKA Analytical). Negative controls included omission of the primary antibody and tissue from animals that had not received BrdU.

Each tumour section was scanned at low power (×100) in order to identify two peripheral areas of tumour with the highest density of BrdU-positive tumour cells. The total number of BrdU-positive and BrdU-negative tumour cells was counted in the two 'hotspots' at ×600 magnification (high-power field; hpf) by a single observer blinded to the treatment allocation of each section. Cell counting was undertaken only if the individual section contained a minimum of two complete hpfs. The proliferation index (PI) was calculated as the % number of BrdU-positive cells counted.

Measurement of tumour apoptosis index

Immunohistochemistry for cleaved caspase-3 was performed as described earlier, except that sections were incubated with 1:100 rabbit anti-activated caspase-3 antibody (Asp175; Cell Signalling Technology Inc., Herts, UK) in Zymed® antibody diluent (Invitrogen) for 60 min. Sections were visualized using the anti-rabbit Envision™ system (DakoCytomation Ltd).

Each tumour section was scanned at ×100 magnification in order to identify two areas of tumour with the highest number of activated caspase (AC)-3-positive tumour cells. The total number of AC-3-positive and AC-3-negative tumour cells was counted in these areas at ×200 magnification by a single observer blinded to the treatment allocation of each section. Cell counting was undertaken only if a section contained a minimum of two complete tumour fields of view for assessment. The apoptosis index (AI) was calculated as the % number of AC-3-positive cells counted.

Immunohistochemistry for phospho-ERK 1/2

Immunohistochemistry for phosphorylated (p) ERK1/2 was carried out as described earlier, except that sections were incubated with a 1:100 dilution of rabbit polyclonal anti-pERK1/2 (threonine 202, tyrosine 204) antibody from Cell Signalling Technology in Zymed® antibody diluent for 60 min at room temperature. Sections were visualized using the anti-rabbit Envision™ system (DakoCytomation Ltd). Staining extent and intensity values at the tumour margin were determined as the mean of 4 random × 20 fields of view scored on a scale of 0 to 3, in which 0 represented no staining and 3 represented the strongest staining intensity of cells at the periphery of tumours. A single observer, who was blinded to the treatment allocation of each section, performed the scoring.

Immunohistochemistry for COX-2

The method used was as described for pERK1/2 immunohistochemistry except that primary rabbit polyclonal anti-COX-2 antibody (Cayman Chemical Co., Ann Arbor, MI, USA) was used at a dilution of 1:50. All sections were stained in a single experiment. COX-2 immunoreactivity was scored by one individual, who was blinded to the treatment allocation of each section. Each section was scored 0–3 for intensity (nil, weak, moderate, strong) and 0–3 for extent (0, no positive staining; 1, <25% tumour area; 2, 25–50% tumour area; 3, >50% tumour area) of COX-2 staining and a total COX-2 immunoreactivity score obtained by addition of the intensity and extent scores.

Immunohistochemistry for the EP4 receptor

The method used was as described for pERK1/2 immunohistochemistry except that rabbit polyclonal anti-EP4 receptor antibody (Cayman Chemical Co.) was used at a dilution of 1:500.

Measurement of tumour microvessel density

Sections for CD31 immunohistochemistry underwent antigen retrieval with proteinase K (100 mg in 10 mM TrisHCl pH 7.5, 20 mM $CaCl_2$, 50% glycerol) diluted 1:500 in PBS for 25 min at 37°C and blocking with avidin/biotin agent (Vector Laboratories Ltd). Sections were incubated with a 1:10 dilution of rat anti-mouse CD31 antibody (BD Pharmingen, San Diego, CA, USA) in Zymed® antibody diluent for 2 h at room temperature. Immunoreactivity was visualized with biotinylated rabbit anti-rat immunoglobulin (DakoCytomation Ltd; 1:200 in Zymed® antibody diluent) and streptavidin/biotin horseradish peroxidase complex (Vector Laboratories), both for 30 min at room temperature, followed by incubation with 3,3′-diaminobenzidine tetrahydrochloride solution (DakoCytomation Ltd).

The number of CD31-positive vessels in three 'hotspots' identified at ×100 magnification was counted at ×200 magnification by a single observer who was blinded to the treatment allocation of each section. Vessel counting was undertaken only if a section contained at least two complete tumour fields of view for assessment.

Analysis of hepatic steatosis

Frozen sections of liver were allowed to dry for 15 min before fixation with 10% (w v^{-1}) formal-calcium overnight at room temperature and staining with 0.5% (v v^{-1}) oil red O in propylene glycol (Sigma, Poole, UK).

Steatosis was scored 1–3 based on the degree and extent of steatosis (1, patchy microvesicular steatosis not filling hepatocytes; 2, some confluent areas of marked steatosis but neighbouring normal hepatocytes; 3, diffuse microvesicular steatosis with 'ballooned' hepatocytes). In each case, a consensus score was gained by two observers, who were both blind to the treatment allocation of each section.

Immunoblot analysis

Snap frozen tissues were lysed in ice-cold RIPA buffer (Sigma) as described previously (Hawcroft *et al.*, 2010) and passed through a QIAshredder homogenizer (QIAGEN Ltd, Crawley, UK). Total protein lysates (50 μg) were separated on a 12% NuPAGE gel (Invitrogen) and then wet-transferred to polyvinylidene fluoride membranes. Membranes were blocked in PBS containing 0.05% (v v^{-1}) NP-40 and 5% (w v^{-1}) milk for 60 min before incubation with rabbit polyclonal anti-COX-2 antibody (Cayman Chemical Co.) diluted 1:250 in PBS containing 0.05% (v v^{-1}) NP-40 and 1% (w v^{-1}) milk and anti-β-actin antibody (Sigma) diluted 1:2000 in PBS containing 0.05% (v v^{-1}) NP-40 and 1% (w v^{-1}) milk, both overnight at 4°C. Membranes were washed 3 × 10 min in PBS containing 0.05% (v v^{-1}) NP-40 followed by 60 min incubation with the appropriate peroxidase-conjugated secondary antibody (DakoCytomation Ltd) at 1:2000 dilution in PBS containing 0.05% (v v^{-1}) NP-40 and 1% (w v^{-1}) milk at room temperature. Following 3 × 10 min washes with PBS-NP40 (0.05%), membranes were visualized using Supersignal West Pico Chemiluminescence kit (Pierce, Rockford, IL, USA) following the manufacturer's instructions. Membranes were imaged using a GelDoc system and Quantity One software (Bio-Rad, Hercules, CA, USA).

MC-26 mouse CRC cell motility assay

Ninety-nine per cent pure EPA-FFA for *in vitro* studies was obtained from SLA Pharma AG. EPA-FFA was dissolved in absolute ethanol carrier at a 1:100 (v v^{-1}) dilution as described previously (Hawcroft *et al.*, 2010).

MC-26 cells were grown to exponential phase and treated with 50 to 200 μM EPA-FFA for 24 h in the presence or absence of 10 μM PGE_2 [from a 10 mM stock solution in dimethyl sulphoxide (DMSO)] or 1 μM PGE_1-alcohol (1 mM stock solution in DMSO; both Cayman Chemical Co.). ONO-AE3-208 (stock solution 1 mM in DMSO) was a kind gift from ONO Pharmaceutical Co. (Osaka, Japan). PD98,059 (stock solution 30 mM in DMSO) was obtained from Calbiochem (Nottingham, UK). Cells were then harvested and counted; 7.5×10^5 cells were seeded in serum-free culture medium in the upper chamber of an 8 μm pore Transwell® insert in the wells of 6 well plate containing a glass coverslip. Medium containing 10% FBS and 5 ng·mL^{-1} recombinant mouse TGF β_1 (PeproTech EC Ltd, London, UK) was added to the lower chamber. Cells were allowed to migrate for 24 h. Cells migrated onto the coverslips were methanol-fixed, stained with haematoxylin and counted from three random ×4 magnification fields of view.

EPA-FFA chemosensitivity assay

The effect of EPA-FFA on MC-26 mouse CRC cell viability *in vitro* was determined using a MTT assay. Briefly, 1×10^3 cells per well were seeded in 96-well plates in 200 μL medium per well and incubated overnight at 37°C. The following day, medium was removed and replaced with fresh medium containing EPA-FFA. Cells were exposed to a range of EPA-FFA concentrations for 24 h, after which they were washed twice with PBS before the addition of fresh medium containing EPA-FFA as appropriate. Following 3 days incubation at 37°C, differences in cell viability were determined using the MTT assay. The IC_{50} was calculated as the mean ± SD of three independent experiments.

Statistical analysis

The significance of differences between treatment groups was tested by either the Mann–Whitney *U*-test and Kruskal–Wallis test for non-parametric data, or Student's *t*-test and one-way ANOVA, with *post hoc* analysis by the Bonferroni method, for normally distributed data. The significance of differences in food intake over time in the treatment groups was analysed by repeated measures ANOVA. The relationships between biomarkers of PUFA incorporation, PG synthesis and tumour growth were analysed by the two-tailed Spearman correlation test. Significance was assumed if the *P* value was less than 0.05.

Results

Administration of 5% EPA-FFA reduces growth of MC-26 mouse CRC cell liver tumours

All mice developed one or more liver metastases after intrasplenic injection of MC-26 mouse CRC cells. The tumour burden consisted of either multiple, small metastases throughout the liver parenchyma (Figure 1A) or a smaller number of discrete tumours, which often extended into the liver hilum (Figure 1B). Liver weight was used as the primary measure of the degree of MC-26 mouse CRC cell liver metastasis. Liver weight was significantly lower in mice that received a 5% EPA-FFA-containing diet [median 1.03 (range 0.59–3.91) g] compared with control animals [median 1.62 (range 0.91–3.40) g; $P = 0.034$; Figure 1C]. There was no significant difference in liver weight between the 2.5% EPA-FFA-treated group [median 1.50 (range 1.05–3.94) g] and controls (Figure 1C). Dietary intake was monitored daily and did not differ significantly between the treatment groups before or after MC-26 mouse CRC cell injection (Supporting Information Figure S1). Although body weight remained stable in all three groups before the intrasplenic injection, there was a decrease in body weight in each group from day 15 onwards, which was most pronounced, but was not significantly different from the control group at killing, in the 5% EPA-FFA-treated animals (Supporting Information Figure S1). As reduced body weight and differences in the time to scheduled killing (four mice in the 5% EPA-FFA-treated group were killed

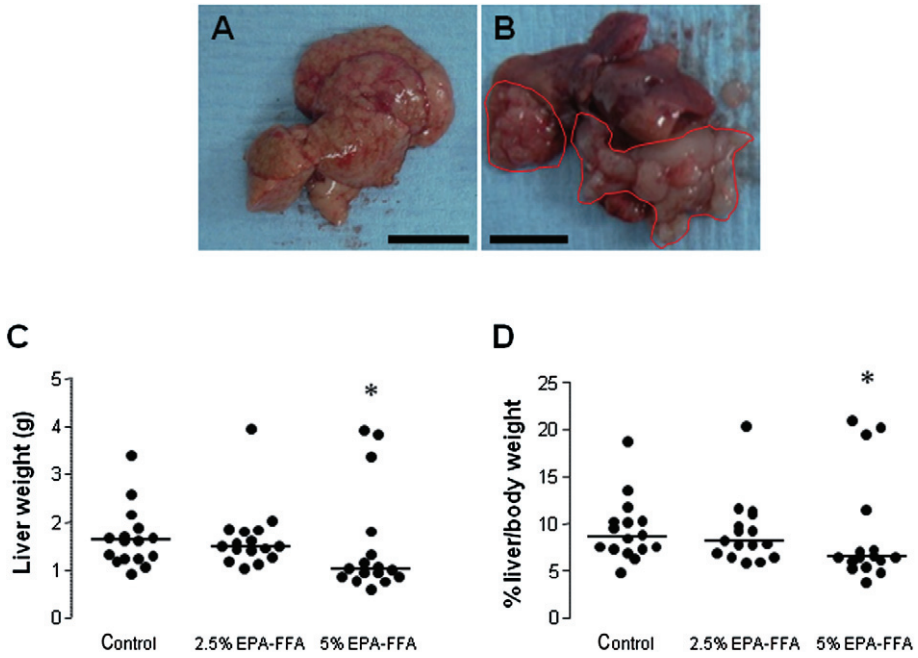

Figure 1

Dietary EPA-FFA administration is associated with reduced growth of MC-26 mouse CRC cell liver metastases. (A,B) Macroscopic appearance of MC-26 mouse CRC cell liver metastases as either multiple small tumour foci throughout the liver (A; size bar = 10 mm) or a smaller number of larger, discrete tumours (highlighted in red) often involving the hilar region (B; size bar = 10 mm). (C) Individual liver weight values at killing. Bars represent the median value for each dietary group (control, $n = 16$; 2.5% EPA-FFA, $n = 16$; 5% EPA-FFA, $n = 16$). *$P = 0.034$ for the comparison between the 5% EPA-FFA-treated and control group; Kruskal–Wallis test. (D) Individual liver/body weight ratios at killing. Bars represent the median value for each dietary group (control, $n = 16$; 2.5% EPA-FFA, $n = 16$; 5% EPA-FFA, $n = 16$). *$P = 0.13$ for the comparison between the 5% EPA-FFA-treated and control group; Kruskal–Wallis *U*-test.

early between days 10 and 13 post-injection due to general ill health rather than at day 15) could confound the use of liver weight as a surrogate end point for liver tumour burden, we also compared liver weight as a percentage of the total body weight between the three intervention groups. Administration of the 5% EPA-FFA-containing diet was also associated with a lower liver/body weight ratio (median 6.5%) compared with control animals (median 8.6%; $P = 0.13$; Figure 1D).

Consistent with the *BALB/c AnN* background (which is related to the *BALB/cByJ* substrain) of the test animals (Lin *et al.*, 2005), we noted a variable degree of steatosis in hepatocytes surrounding tumour tissue in all animals (Supporting Information Figure S2). However, the extent of fatty change did not differ between EPA-FFA-treated and control animals (Supporting Information Figure S2). There was no evidence of steatohepatitis in any liver specimen.

Dietary EPA-FFA is incorporated into MC-26 mouse CRC cell liver tumours

Based on previous data from rodent CRC models (Calder *et al.*, 1998; Boudreau *et al.*, 2001; Togni *et al.*, 2003), we hypothesized that orally administered EPA-FFA would be incorporated into MC-26 mouse CRC cell tumours leading to an increase in tissue EPA content at the expense of the ω-6 PUFA AA. MC-26 mouse CRC cell tumour tissue from control *BALB/c* mice contained relatively low levels of EPA [mean relative content 0.14 ± 0.04% (SEM)] with correspondingly higher levels of AA (10.1 ± 0.84%; Figure 2A). Administration of 2.5% EPA-FFA in the diet was associated with a slight increase in tumour EPA content (to 0.43 ± 0.08%) and a larger, but statistically insignificant, reduction in AA to a relative content of 7.26 ± 1.13% ($P = 0.09$; Figure 2A). By contrast, tumour tissue from animals, which received 5% EPA-FFA, contained higher relative levels of EPA (3.68 ± 0.81%; $P < 0.001$ compared with control and 2.5% EPA-FFA-treated groups), with a statistically significant reduction in AA content to 4.63 ± 0.54% ($P = 0.01$ for the comparison with control tumour tissue; Figure 2A). At the higher dietary dose of EPA-FFA, there was a simultaneous increase in levels of docosapentaenoic acid (DPA) in tumour tissue, but not of DHA, suggesting that EPA-DHA conversion does not occur to any significant extent in these CRC cell tumours with the limiting step being (DPA to DHA) reductase activity (Figure 2A). Expressed as the EPA/AA ratio, there was a dose-dependent increase in the EPA/AA ratio associated with EPA-FFA administration with the tumour EPA/AA ratio approximating the value 1 in mice administered 5% EPA-FFA (Figure 2C). As expected, similar ω-3 PUFA levels and differences in the relative content of EPA and AA related to EPA-FFA treatment were observed in neighbouring liver tissue (Figure 2B). In addition, the relative DHA content of the liver was noted to be higher in all three treatment groups than that in MC-26 mouse CRC cell tumour tissue (Figure 2B).

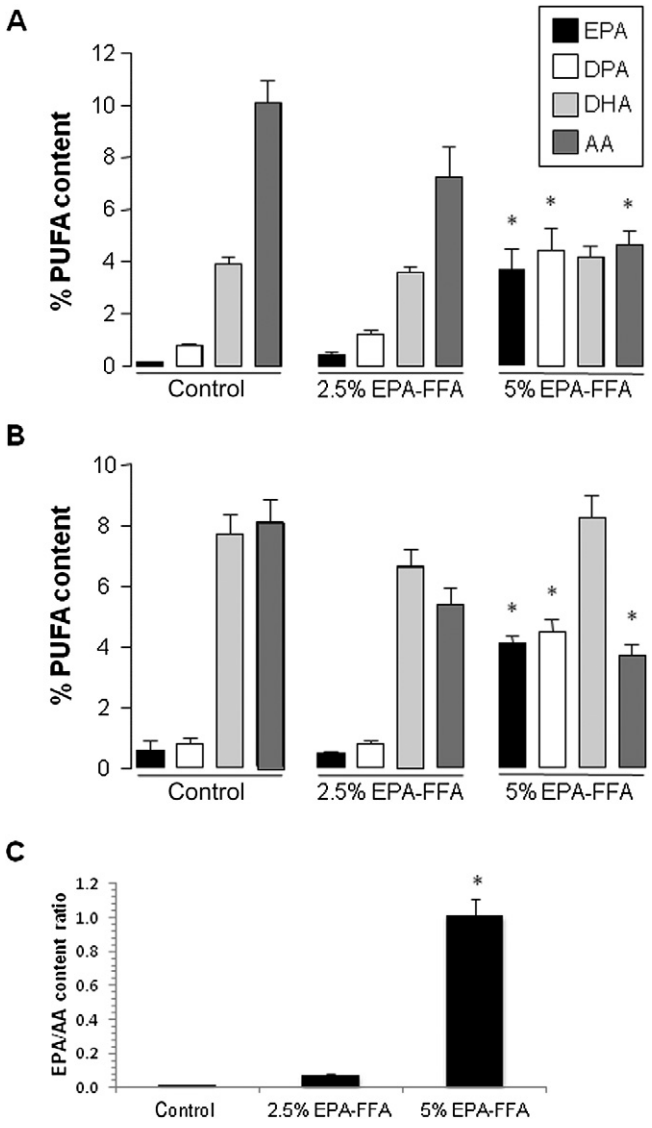

Figure 2

Changes in PUFA content of MC-26 mouse CRC cell liver tumours and liver tissue associated with EPA-FFA administration. The relative (% total) PUFA content of MC-26 mouse CRC cell tumour tissue (A) and neighbouring liver tissue (B) after exposure to either control or EPA-FFA-containing diets for 28 days. Columns and bars represent the mean and the SEM, respectively, for $n = 14$ (control and 2.5% EPA-FFA) and $n = 10$ (5% EPA-FFA) tumours, as well as $n = 16$ (control and 2.5% EPA-FFA) and $n = 14$ (5% EPA-FFA) liver samples. *$P < 0.01$ compared with the control group; one-way ANOVA with *post hoc* Bonferroni analysis. (C) The EPA/AA ratio of MC-26 mouse CRC cell tumour tissue in the three dietary groups. Columns and bars represent the mean and the SD respectively. *$P < 0.05$ for the comparison between the 5% EPA-FFA-treated group with control and 2.5% EPA-FFA-treated animals (one-way ANOVA with *post hoc* Bonferroni analysis).

Dietary EPA-FFA administration is associated with reduced PGE_2 levels and PGE_3 synthesis in MC-26 mouse CRC cell liver metastases

In the absence of dietary EPA-FFA supplementation, MC-26 mouse CRC cell liver tumours contained high levels of PGE_2 [mean 5970 ± 711 (SEM) $pg \cdot mg^{-1}$ wet weight tissue] compared with normal liver tissue (Figure 3A,B). This is consistent with known constitutive COX-2 expression and COX-2-dependent PGE_2 production by MC-26 mouse CRC cells *in vitro* (Pozzi *et al.*, 2004; Hawcroft *et al.*, 2010). Administration of 2.5% EPA-FFA in the diet was not associated with any significant change in intra-tumoural PGE_2 content (Figure 3A). However, exposure to 5% EPA-FFA in the diet was associated with a significant, 60%, decrease in intratumoural PGE_2 levels compared with control liver metastases ($P = 0.006$; Figure 3A). In addition, EPA-FFA administration was associated with a significant dose-dependent increase in PGE_3 in MC-26 mouse CRC cell liver tumour tissue (Figure 3A). PGE_3 levels were an order of magnitude lower than corresponding tissue PGE_2 levels reaching 321 ± 59 $pg \cdot mg^{-1}$ in tumours from 5% EPA-FFA-treated animals (Figure 3A). Despite the reduction in tumour PGE_2 content of 5% EPA-FFA-treated tumour tissue, no significant difference in tumour COX-2 protein levels between control and 5% EPA-FFA-treated tumours was observed by Western blot analysis or immunohistochemistry (Figure 3C,D and Supporting Information Figure S3).

Although changes in PUFA content related to EPA-FFA administration, similar to those noted in tumour tissue, were observed in the liver (Figure 3B), no significant difference in PGE_2 levels was observed in the liver of EPA-FFA-treated mice compared with control animals (Figure 3B). Only very low levels of PGE_3 were detected in normal liver tissue from EPA-FFA-treated animals compared with metastasis tissue (Figure 3B).

We hypothesized that changes in the PUFA content of tumour tissue from individual animals would predict the observed differences in E-type PG levels from the same mice. There was a weak, but statistically significant, negative correlation between the EPA/AA ratio and PGE_2 level, as well as a stronger positive correlation between the EPA/AA ratio and PGE_3 level, in individual tumours (Supporting Information Figure S3). Interestingly, there appeared to be a threshold EPA/AA ratio value (approximately 0.1), above which MC-26 CRC cell tumour PGE_3 synthesis occurred (Supporting Information Figure S4). Moreover, there was a weak, but statistically significant, negative correlation between the EPA/AA ratio and liver tumour burden as measured by liver weight. However, differences in the individual tumour EPA/AA ratio did not explain the small number of outlier cases in the three experimental groups with a large tumour burden (compare Figure 1 and Supporting Information Figure S4).

Dietary EPA-FFA administration decreases MC-26 mouse CRC cell proliferation

We next sought a mechanistic explanation for the reduced liver tumour growth in 5% EPA-FFA-treated animals. Reduction of PGE_2 content and CRC cell proliferation (measured by Ki-67 immunohistochemistry) has previously been reported in EPA-treated HT-29 human CRC cell xenograft tumours in nude mice (Calviello *et al.*, 2004). Therefore, we measured the % number of BrdU-positive tumour cells (the PI) in liver metastasis tissue. Treatment with 5% EPA-FFA was associated with a statistically significant, overall 19%, lower tumour PI than control tumour tissue ($P = 0.04$; Figure 4A). Consistent

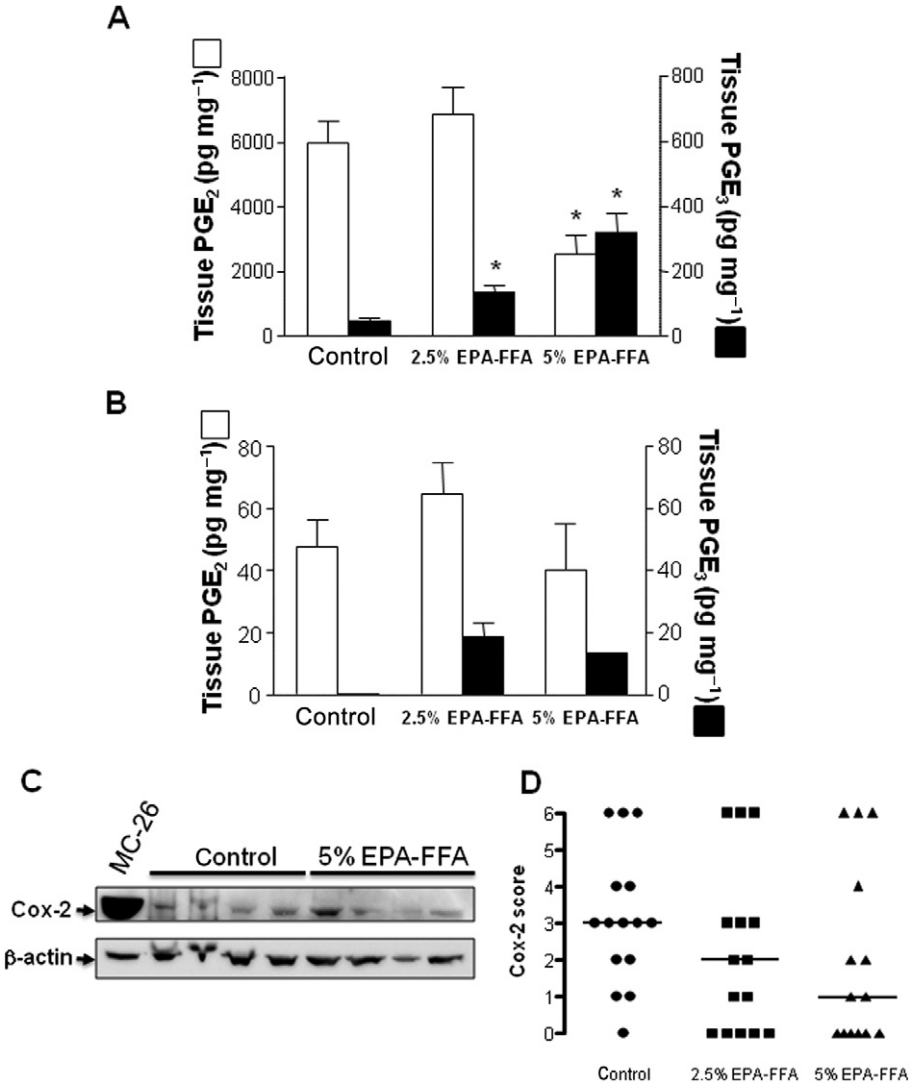

Figure 3

EPA-FFA administration leads to changes in E-type PG levels in MC-26 mouse CRC cell tumour tissue. PGE_2 (open columns) and PGE_3 (solid columns) levels in (A) MC-26 mouse CRC cell tumour tissue [n = 15 (control), n = 14 (2.5% EPA-FFA) and n = 7 (5% EPA-FFA)] and (B) neighbouring liver tissue [n = 10 (control), n = 13 (2.5% EPA-FFA) and n = 5 (5% EPA-FFA)] after exposure to either control or EPA-FFA-containing diets for 28 days. Columns and bars represent the mean and SEM, respectively. *P < 0.05; one-way ANOVA with *post hoc* Bonferroni analysis. (C) Western blot analysis of COX-2 protein in tumour tissue from control (n = 4) and 5% EPA-FFA-treated (n = 4) animals. In each case, 50 μg total protein was loaded. β-actin was probed as a loading control. MC-26 denotes a total protein sample from MC-26 mouse CRC cells cultured *in vitro*. Densitometry confirmed that there was no significant difference in the COX-2/β-actin ratio between control tumour tissue [mean ratio 5.5 ± 0.4 (SEM) arbitrary units] and tumour tissue from 5% EPA-FFA-treated animals (7.0 ± 1.1 arbitrary units; P = 0.56, Mann–Whitney U-test). (D) Immunohistochemistry for COX-2 in tumour tissue from control (n = 15), 2.5% EPA-FFA-treated (n = 15) and 5% EPA-FFA-treated (n = 14) animals. Data points represent individual COX-2 immunoreactivity scores (see Supporting Information Figure S3) and bars denote median values for each group. There was no significant difference in COX-2 immunoreactivity scores between the treatment groups (P = 0.16; Kruskal–Wallis test).

with the lack of effect of 2.5% EPA-FFA administration on tumour size and PGE_2 synthesis, the tumour PI in the 2.5% EPA-FFA-treated group was not significantly different from the PI of control tumour tissue (Figure 4A).

By contrast, EPA-FFA did not induce MC-26 mouse CRC cell apoptosis in metastatic liver tumours (Figure 4B), nor was there any significant difference in CD31-positive microvessel density between the three treatment groups (Figure 4C).

Dietary EPA-FFA administration decreases MC-26 mouse CRC cell ERK signalling at the tumour periphery in vivo *and EPA-FFA decreases MC-26 mouse CRC cell motility* in vitro

ERK signalling occurs downstream of PGE_2-induced activation of the EP_4 (but not EP_2) receptor (Fujino *et al.*, 2003; Pozzi

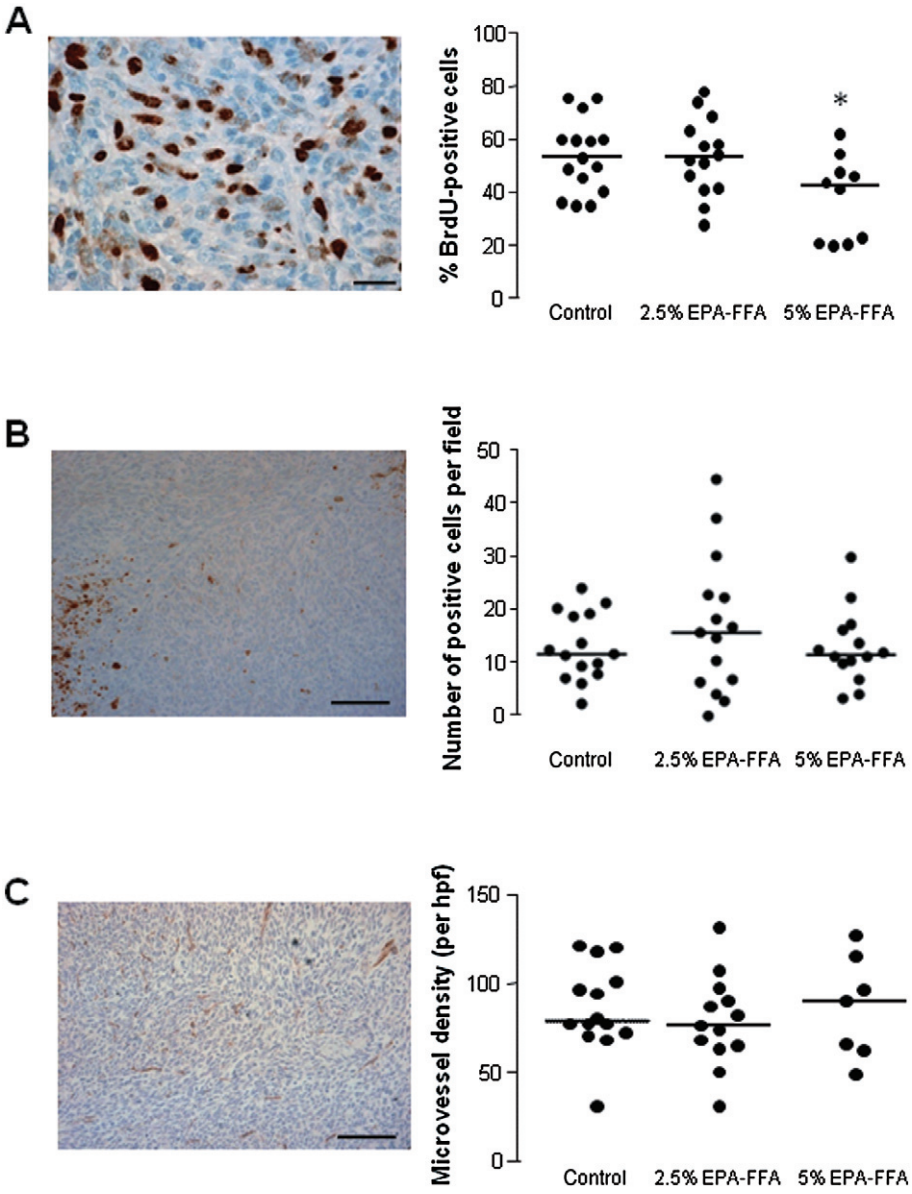

Figure 4

Biomarkers of MC-26 mouse CRC cell tumour growth in control and EPA-FFA-treated animals. (A) Immunohistochemistry for BrdU: a representative photomicrograph demonstrating brown BrdU-positive MC-26 mouse CRC cells in liver metastasis tissue (size bar = 20 μm) and individual BrdU proliferation index (PI) values in the three treatment groups [$n = 16$ (control), $n = 14$ (2.5% EPA-FFA), $n = 12$ (5% EPA-FFA)]. Bars represent the median value. *$P = 0.04$ for the comparison with control tumour PI values (Kruskal–Wallis test). (B) Immunohistochemistry for activated caspase-3 (AC-3): a representative photomicrograph (size bar = 100 μm) demonstrating individual brown AC-3-positive MC-26 cells within tumours. Focal areas of high AC-3-positivity were noted in both control and EPA-FFA-treated tumours. Individual AC-3 apoptosis index values in the three treatment groups are presented in the accompanying figure [$n = 15$ (control), $n = 15$ (2.5% EPA-FFA), $n = 14$ (5% EPA-FFA)]. Bars represent the median value. (C) Immunohistochemistry for CD31: a representative photomicrograph of CD31-positive vessels in a MC-26 mouse CRC cell liver tumour (size bar = 100 μm) and individual CD31-positive microvessel density values in the three treatment groups [$n = 14$ (control), $n = 14$ (2.5% EPA-FFA), $n = 7$ (5% EPA-FFA)]. Bars represent the median value.

et al., 2004; Hawcroft *et al.*, 2007). Moreover, EPA has been demonstrated to reduce pERK levels in human CRC cells *in vitro* (Calviello *et al.*, 2004). Therefore, pERK1/2 localization and levels in MC-26 mouse CRC cell tumours *in vivo* were determined by immunohistochemistry. pERK1/2 immunoreactivity was restricted to the periphery of tumours, particularly those at the leading edge of the tumour, suggesting a link with cell invasion and motility at the expanding edge of tumours (Figure 5A–D). EP_4 receptor immunoreactivity was more widespread and was present throughout MC-26 mouse CRC cell tumours (Figure 5E–F). However, staining was strongest at the periphery of liver metastases, in a similar distribution to pERK1/2 staining (Figure 5E–F). The intensity and extent of pERK1/2 staining at the tumour margin was

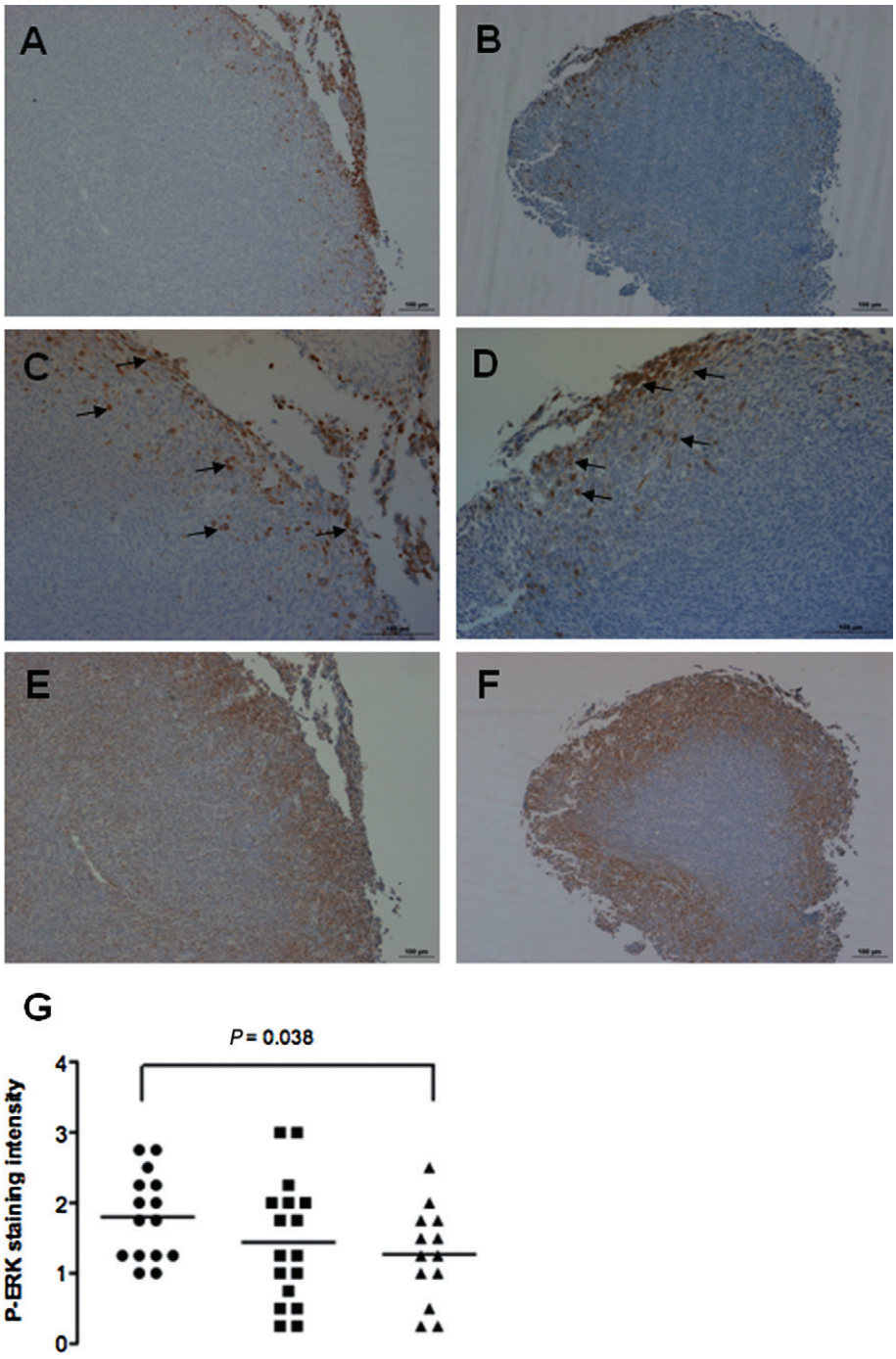

Figure 5

pERK1/2 immunoreactivity in MC-26 mouse CRC cell tumours is reduced in 5% EPA-FFA-treated animals. Representative low- (A,B) and high-power (C,D) photomicrographs of pERK1/2 staining at the periphery of tumours from control (A,C) or 5% EPA-FFA-treated (B,D) animals. Examples of pERK-positive cells at the invading edge of the tumours are highlighted by arrows. Size bars = 100 μm. (E) and (F) Representative photomicrographs of EP_4 receptor staining in the same tumours as above from control (E) or 5% EPA-FFA-treated (F) animals. EP_4 receptor immunoreactivity was present throughout MC-26 mouse CRC cells tumours but was most prominent at the periphery of the tumour in a similar distribution to pERK1/2 staining. Size bars = 100 μm. (G) Individual pERK1/2 scores of liver tumours from the three treatment groups [n = 15 (control), n = 16 (2.5% EPA-FFA), n = 13 (5% EPA-FFA)]. Bars represent the median value. *P = 0.038 for the comparison between the 5% EPA-FFA-treated and control groups, Student's unpaired t-test.

significantly lower in animals on a 5% EPA-FFA-containing diet [mean pERK1/2 score 1.3 ± 0.19 (SD)] compared with the control group (1.8 ± 0.16; $P = 0.038$; Figure 5G). However, there was no discernable difference in EP_4 receptor immunoreactivity in tumours from animals on a 5% EPA-FFA-containing diet compared with controls (Figure 5E–F).

Given a potential link between ERK1/2 activation and invasion at the edge of MC-26 mouse CRC cell liver tumours, we hypothesized that EPA-FFA reduced CRC liver metastasis growth via attenuation of MC-26 mouse CRC cell motility. MC-26 cells migrated through an 8 μm pore towards a chemotactic $TGF\beta_1$ signal within 24 h (Figure 6A). Pretreatment with EPA-FFA for 24 h before seeding of cells onto a Transwell® membrane decreased MC-26 mouse CRC cell migration in a dose-dependent manner (Figure 6B–D,G), with 200 μM EPA-FFA [similar to the IC_{50} for EPA-FFA in a MTT assay (Supporting Information Figure S5)] causing an approximate threefold reduction in MC-26 mouse CRC cell motility (Figure 6G). Importantly, incubation with 10 μM PGE_2 [a concentration similar to PGE_2 levels obtained in MC-26 cell-conditioned medium (Hawcroft *et al.*, 2010)] for 24 h rescued the effect of EPA-FFA on MC-26 mouse CRC cells (Figure 6G,H), thus providing evidence that inhibition of PGE_2 synthesis, at least partly, explains the effect of EPA-FFA on MC-26 mouse CRC cell motility. An attractive hypothesis linking PGE_2-dependent effects of EPA-FFA on cell motility *in vitro* and the similar localization of pERK1/2 and the EP_4 receptor in MC-26 mouse CRC cell liver tumours *in vivo* is that EPA-FFA attenuates PGE_2-EP_4 receptor-dependent cell migration. Consistent with this notion, the specific EP_4 receptor antagonist ONO-AE3-208 (Hawcroft *et al.*, 2007) mimicked the effect of EPA-FFA in the Transwell® cell migration assay (Figure 6H), as did the mitogen-activated ERK kinase 1/2 inhibitor PD98,059 (Figure 6H). Importantly, PGE_1-alcohol [used at a concentration (1 μM) at which it retains properties as a specific EP_4 receptor agonist (Kiriyama *et al.*, 1997)] rescued the effect of EPA-FFA on migration of MC-26 mouse CRC cells suggesting that a reduction of PGE_2-EP_4 receptor signalling contributes to the antineoplastic activity of EPA-FFA (Figure 6H).

Discussion

This is the first study to demonstrate anti-CRC efficacy and gain new mechanistic insights into the antineoplastic activity of an ω-3 PUFA in a pre-clinical model of CRC liver metastasis. Our data add to a body of evidence that EPA has direct anti-CRC activity relevant to treatment of established CRC (Cockbain *et al.*, 2012) and implicate a reduction in PGE_2-mediated tumour cell invasion in the anti-CRC activity of EPA-FFA in the MC-26 mouse CRC cell liver metastasis model.

We acknowledge that we tested high daily doses of EPA-FFA (roughly equivalent to 12 $g \cdot Kg^{-1}$ mouse weight based on daily food intake during the experiment) in order to accentuate the antineoplastic activity of EPA-FFA and permit detailed mechanistic studies. The dose range that was tested was the same as that previously employed by Fini *et al.* (2010) and was similar to dosing of fish oil preparations in previous rodent models of CRC (Cockbain *et al.*, 2012). The premature mortality observed in the 5% (w w^{-1}) group is unexplained but was not related to increased tumour burden.

We have confirmed that oral administration of the FFA form of EPA leads to incorporation of EPA into metastatic tumour tissue and surrounding normal liver at levels similar to those obtained in rectal mucosa with chronic (6 month) dosing with EPA-FFA in humans (West *et al.*, 2010). The concurrent reduction in the relative content of AA that we observed has been reported previously in other rodent CRC cell models (Calder *et al.*, 1998; Boudreau *et al.*, 2001; Togni *et al.*, 2003). In the *BALB/c* mouse, significant tissue incorporation of EPA only occurred at the higher EPA-FFA dose suggesting there may be strain- and/or organ-specific differences in efficiency of membrane EPA incorporation in comparison with *C57/Bl6* mouse intestine (Fini *et al.*, 2010). We also noted a significantly higher relative content of DHA in host liver compared with neighbouring MC-26 mouse CRC cell tumour tissue, consistent with the lower DHA content of rectal epithelium compared with liver in humans (Arteburn *et al.*, 2006).

An important landmark finding of this study is that oral EPA administration leads to a 'PGE_2-to-PGE_3 switch' in CRC tissue *in vivo*. Previous observations of this phenomenon had been restricted to human cancer cells *in vitro* (Yang *et al.*, 2004; Hawcroft *et al.*, 2010) and normal colorectal mucosa in mice (Vanamala *et al.*, 2008). A significant reduction in tissue PGE_2 levels and evidence of *de novo* PGE_3 synthesis occurred only in the group of animals, in which EPA-FFA [at 5% (w w^{-1})] demonstrated antineoplastic activity. The results of an equivalent PG analysis in human CRC liver metastasis tissue from an ongoing Phase II RCT of EPA-FFA should determine the potential utility of E-type PGs [or stable metabolites such as urinary PGE-M (Murphey *et al.*, 2004)] as therapeutic response biomarkers for ω-3 PUFA therapy. The relative contributions to the antineoplastic activity of EPA of the reduction in PGE_2 content versus appearance of PGE_3, which can both lead to reduction in pro-tumourigenic EP_4 receptor activation (Hawcroft *et al.*, 2010), remains to be determined.

The absence of any significant reduction in PGE_2 levels in neighbouring normal liver tissue, despite equivalent incorporation of EPA to that observed in tumour tissue, suggests that EPA-mediated effects on E-type PG synthesis were tumour-specific and were explained by modulation of dominant MC-26 cell COX-2 activity [as is recognized *in vitro* (Hawcroft *et al.*, 2010)], with little or no inhibition of constitutive hepatic PGE_2 synthesis, which is likely to be driven largely by COX-1.

We did not obtain any definitive evidence of a reduction in COX-2 expression in MC-26 mouse CRC cells by EPA *in vivo* by either Western blot analysis or immunohistochemistry. There was a trend towards reduced COX-2 immunoreactivity in fixed tissue sections of EPA-FFA-treated tumours, which requires further investigation, particularly as immunohistochemical findings can be highly antibody-dependent (Garewal *et al.*, 2003). By contrast, EPA exposure has previously been associated with reduced COX-2 protein levels in HT-29 human CRC cells (Calviello *et al.*, 2004). In our experiments, it remains likely that the large reduction in PGE_2 levels observed in MC-26 mouse CRC cell tumours is explained predominantly by modulation of COX-2 enzymatic activity

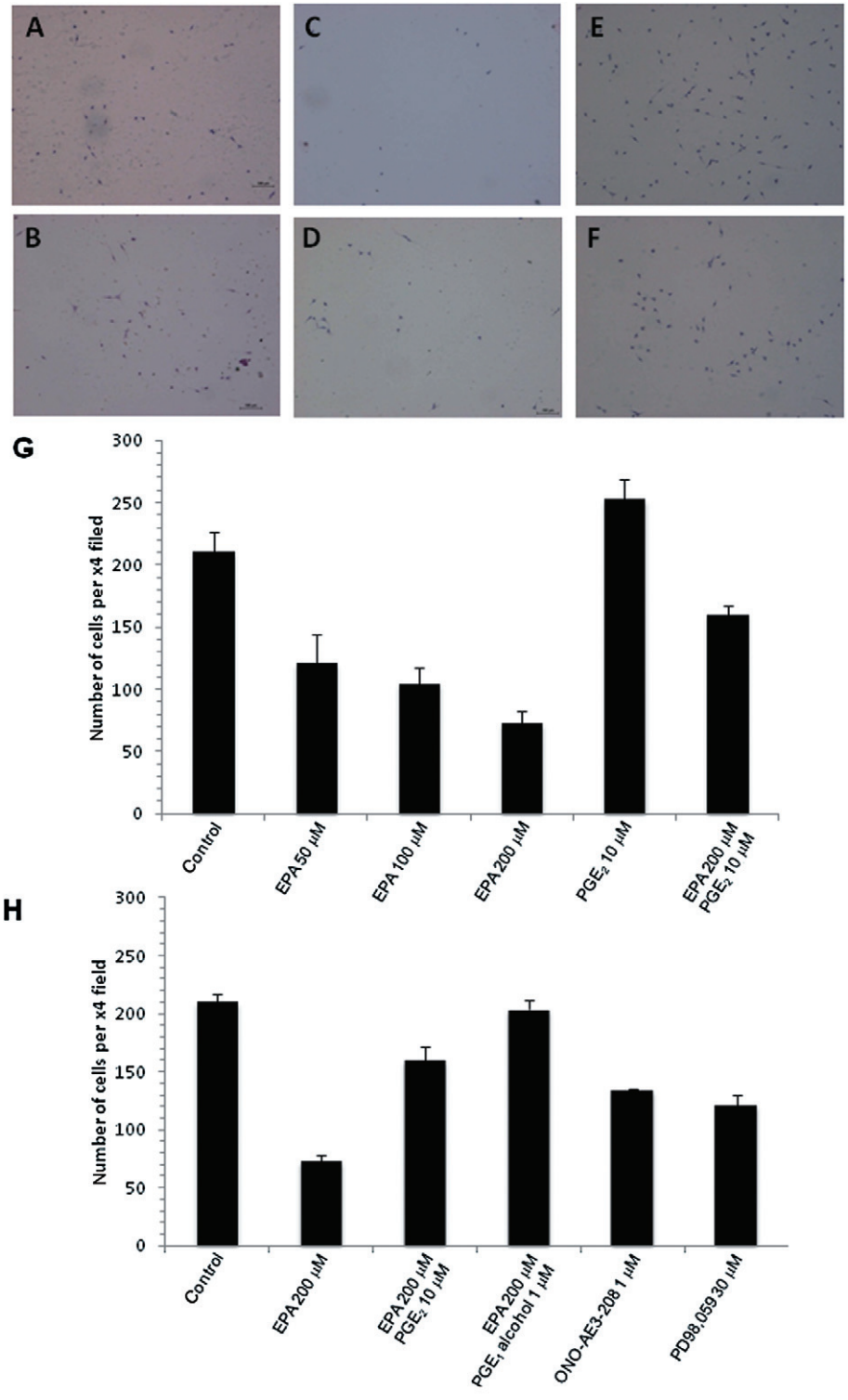

Figure 6

Effect of EPA-FFA on MC-26 mouse CRC cell motility *in vitro*. (A to F) Representative photomicrographs of cells following migration through 8 μm membrane pores. Images of control cells (A) and cells treated with either 50 μM (B), 100 μM (C), 200 μM EPA-FFA (D), 10 μM PGE_2 alone (E) or a combination of 200 μM EPA-FFA and 10 μM PGE_2 (F). (G) Quantification of the effect of EPA-FFA on MC-26 mouse CRC cell migration. Data are expressed as the mean and SEM of the number of cells counted per ×4 magnification field of view from a minimum of three replicates. (H) Quantification of MC-26 mouse CRC cell migration. Data are expressed as the mean and SEM of the number of cells counted per ×4 magnification field of view from a minimum of four replicates.

rather than alterations in COX-2 expression in MC-26 mouse CRC cells.

A reduction in the PI of 5% EPA-FFA-treated MC-26 mouse CRC cell liver tumours is consistent with observations made in the one previous study that measured the PI in EPA-treated human CRC cell xenograft tumours by Ki-67 immunostaining (Calviello *et al.*, 2004). The modest reduction (approximately 20%) in PI that we observed is compatible with biologically significant effects of ω-3 PUFAs on colorectal carcinogenesis in other pre-clinical models (Deschner *et al.*, 1990; Hendrickse *et al.*, 1995; Latham *et al.*, 1999), as well as clinically relevant effects of established anticancer agents against human CRC liver metastases (Backus *et al.*, 2001; Zhong *et al.*, 2008) and other malignancies (Clarke *et al.*, 1993).

A striking observation was that ERK signalling in MC-26 mouse CRC cell tumours was restricted to cancer cells at the leading or invasive edge of the tumour where pERK protein was localized by immunohistochemistry. This is consistent with a previous report of the critical role of ERK signalling in TNFα-induced MC-26 mouse CRC cell invasion and metastasis (Choo *et al.*, 2005). There are several potential mechanisms that could explain how EPA could reduce ERK activation in CRC cells. Firstly, it is known that ERK signalling occurs downstream of EP_4 receptor activation (Fujino *et al.*, 2003; Pozzi *et al.*, 2004; Hawcroft *et al.*, 2007). Therefore, the EPA-induced reduction in PGE_2-EP_4 receptor signalling may account for reduced pERK levels in the MC-26 mouse CRC cell tumours. Alternatively, ω-3 PUFAs are believed to alter membrane dynamics, particularly lipid raft function (Cockbain *et al.*, 2012), which could affect cell surface receptor (e.g. EGF receptor) function upstream of the ERK signalling pathway. It should be noted that MC-26 mouse CRC cells do not express EGF receptors (M. Volpato, unpubl. data and Lee *et al.*, 2010) so that effects on CRC cell EGF receptor activity cannot explain EPA-FFA activity in this model.

Reduced pERK levels in CRC cells at the edge of liver tumours in animals treated with EPA-FFA-containing diet, combined with the known role of ERK signalling in CRC cell invasiveness (Choo *et al.*, 2005; Rao *et al.*, 2007), led us to test whether EPA-FFA decreased CRC cell motility using an *in vitro* cell migration assay. The concentration-dependent decrease in MC-26 mouse CRC cell motility by EPA-FFA was completely rescued by exogenous PGE_2, thus implicating reduced PGE_2 signalling in this aspect of the antineoplastic activity of EPA-FFA. This was, at least in part, due to reduced PGE_2-EP_4 receptor activation in MC-26 mouse CRC cells based on attenuation of the effect of EPA-FFA on cell migration by the EP_4 receptor ligand PGE_1-alcohol. Differential expression of the EP_4 receptor within CRC cell tumours has not been previously reported and requires further investigation as a factor controlling the antineoplastic activity of agents such as EPA-FFA, which modulate PGE_2 synthesis and signalling.

In summary, we have demonstrated that orally administered EPA, in the FFA form, reduces CRC liver tumour growth in a mouse model of CRC liver metastasis by mechanisms including decreased CRC cell proliferation and reduced PGE_2-dependent cell motility. Currently, a Phase II randomized placebo-controlled trial of EPA-FFA 2 g daily is underway in patients awaiting liver resection surgery for CRC liver metastasis (http://www.clinicaltrials.gov, NCT01070355). Evidence of safety and good tolerability of EPA-FFA in this group of patients with advanced CRC, combined with this pre-clinical evidence of efficacy of EPA-FFA against CRC liver metastasis, should prompt Phase III clinical evaluation of EPA-FFA for prevention and/or treatment of CRC liver metastasis. Definitive evidence that the antineoplastic activity of EPA is, at least partly, explained by reduced PGE_2 bioactivity will lead to evaluation of the stable urinary metabolite of PGE_2 PGE-M as a therapeutic response biomarker in CRC patients receiving EPA therapy (Johnson *et al.*, 2006).

Acknowledgements

This work was supported by Yorkshire Cancer Research, the Medical Research Council (UK) and an unrestricted Scientific Grant from SLA Pharma AG.

Conflict of interest

MH and AB have received unrestricted Scientific Grants and travel grants from SLA Pharma AG. LC has received a travel grant from VisualSonics Inc.

References

Alexander SPH, Mathie A, Peters JA (2011). Guide to Receptors and Channels (GRAC), 5th Edition (2011). Br J Pharmacol 164 (Suppl. 1): S1–S324.

Arteburn LM, Bailey Hall E, Oken H (2006). Distribution, interconversion, and dose response of n-3 fatty acids in humans. Am J Clin Nutr 83 (Suppl.): 1467S–1476S.

Backus HHJ, Dukers DF, van Groeningen CJ, Vos W, Bloemena E, Wouters D *et al.* (2001). 5-Fluorouracil induced Fas upregulation associated with apoptosis in liver metastases of colorectal cancer patients. Ann Oncol 12: 209–216.

Boudreau MD, Sohn KH, Rhee SH, Lee SW, Hunt JD, Hwang DH (2001). Suppression of tumor cell growth both in nude mice and in culture by n-3 polyunsaturated fatty acids: mediation through cyclooxygenase-independent pathways. Cancer Res 61: 1386–1391.

Calder PC, Davis J, Yaqoob P, Pala H, Thies F, Newsholme EA (1998). Dietary fish oil suppresses human colon tumour growth in athymic mice. Clin Sci (Lond) 94: 303–311.

Calviello G, Di Nicuolo F, Gragnoli S, Piccioni E, Serini S, Maggiano N *et al.* (2004). n-3 PUFAs reduce VEGF expression in human colon cancer cells modulating the COX-2/PGE2 induced ERK-1 and -2 and HIF-1alpha induction pathway. Carcinogenesis 25: 2303–2310.

Chapkin RS, McMurray DN, Lupton JR (2007). Colon cancer, fatty acids and anti-inflammatory compounds. Curr Opin Gastroenterol 23: 48–54.

Choo M-K, Sakurai H, Koizimi K, Saiki I (2005). Stimulation of cultured colon 26 cells with TNF-α promotes lung metastasis through the extracellular signal-regulated kinase pathway. Cancer Lett 230: 47–56.

Clarke RB, Laidlaw IJ, Jones LJ, Howell A, Anderson E (1993). Effect of tamoxifen on Ki67 labelling index in human breast tumours and its relationship to oestrogen and progesterone receptor status. Br J Cancer 67: 606–611.

Cockbain AJ, Toogood GJ, Hull MA (2012). Omega-3 polyunsaturated fatty acids for the prevention and treatment of colorectal cancer. Gut 61: 135–149.

Deschner EE, Lytle JS, Wong G, Ruperto JF, Newmark HL (1990). The effect of dietary omega-3 fatty acids (fish oil) on azoxymethanol-induced focal areas of dysplasia and colon tumor incidence. Cancer 66: 2350–2356.

Fini L, Piazzi G, Ceccarelli C, Daoud Y, Belluzzi A, Munarini A *et al.* (2010). Highly purified eicosapentaenoic acid as free fatty acids strongly suppresses polyps in ApcMin/+ mice. Clin Cancer Res 16: 5703–5711.

Fujino H, Xu W, Regan RW (2003). Prostaglandin E2 induced functional expression of early growth response factor-1 by EP4, but not EP2, prostanoid receptors via the phosphatidylinositol 3-kinase and extracellular signal-regulated kinases. J Biol Chem 278: 12151–12156.

Garewal H, Ramsey L, Fass R, Hart NK, Payne CM, Bernstein H *et al.* (2003). Perils of immunohistochemistry: variability in staining specificity of commercially available COX-2 antibodies on human colon tissue. Dig Dis Sci 48: 197–202.

Griffini P, Fehres O, Klieverik L, Vogels IM, Tigchelaar W, Smorenburg SM *et al.* (1998). Dietary omega-3 polyunsaturated fatty acids promote colon carcinoma metastasis in rat liver. Cancer Res 58: 3312–3319.

Gutt CN, Brinkmann L, Mehrabi A, Fonouni H, Müller-Stich BP, Vetter G *et al.* (2007). Dietary omega-3-polyunsaturated fatty acids prevent the development of metastases of colon carcinoma in rat liver. Eur J Nutr 46: 279–285.

Hawcroft G, Ko CWS, Hull MA (2007). Prostaglandin E2-EP4 receptor signalling promotes tumorigenic behaviour of HT-29 human colorectal cancer cells. Oncogene 26: 3006–3019.

Hawcroft G, Loadman PM, Belluzzi A, Hull MA (2010). Effect of eicosapentaenoic acid on E-type prostaglandin synthesis and EP4 receptor signalling in human colorectal cancer cells. Neoplasia 12: 618–627.

Hendrickse CW, Keighley MR, Neoptolemos JP (1995). Dietary omega-3 fats reduce proliferation and tumor yields at colorectal anastomosis in rats. Gastroenterology 109: 431–439.

Hillier K, Jewell R, Dorrell L, Smith CL (1991). Incorporation of fatty acids from fish oil and olive oil into colonic mucosal lipids and effects upon eicosanoid synthesis in inflammatory bowel disease. Gut 32: 1151–1155.

Iwamoto S, Senzaki H, Kiyozuka Y, Ogura E, Takada H, Hioki K *et al.* (1998). Effects of fatty acids on liver metastasis of ACL-15 rat colon cancer cells. Nutr Cancer 31: 143–150.

Johnson JC, Schmidt CR, Shrubsole MJ, Billheimer DD, Joshi PR, Morrow JD *et al.* (2006). Urine PGE-M: a metabolite of prostaglandin E2 as a potential biomarker of advanced colorectal neoplasia. Clin Gastroenterol Hepatol 4: 1358–1365.

Kiriyama M, Ushikubi F, Kobayashi T, Hirata M, Sugimoto Y, Narumiya S (1997). Ligand binding specificities of the eight types and subtypes of the mouse prostanoid receptors expressed in chinese hamster ovary cells. Br J Pharmacol 122: 217–224.

Latham P, Lund EK, Johnson IT (1999). Dietary n-3 PUFA increases the apoptotic response to 1,2-dimethylhydrazine, reduces mitosis and suppresses the induction of carcinogenesis in the rat colon. Carcinogenesis 20: 645–650.

Lawson LD, Hughes BG (1988). Human absorption of fish oil fatty acids as triacylglycerols, free acids, or ethyl esters. Biochem Biophys Res Commun 152: 328–335.

Lee J, Choi Y, Kim K, Hong S, Park H-Y, Lee T *et al.* (2010). Characterization and cancer cell specific binding properties of anti-EGFR antibody conjugated quantum dots. Bioconjug Chem 21: 940–946.

Lin X, Yue P, Chen Z, Schonfeld G (2005). Hepatic triglyceride contents are genetically determined in mice: results of a strain survey. Am J Physiol Gastrointest Liver Physiol 288: G1179–G1189.

Murphey LJ, Williams MK, Sanchez SC, Byrne LM, Csiki I, Oates JA *et al.* (2004). Quantification of the major urinary metabolite of PGE2 by a liquid chromatographic/mass spectrometric assay: determination of cyclooxygenase-specific PGE2 synthesis in healthy humans and those with lung cancer. Anal Biochem 334: 266–275.

Petrik MBH, McEntee MF, Chiu CH, Obukowicz MG, Whelan J (2000). Antagonism of arachidonic acid is linked to the antitumorigenic effect of dietary eicosapentaenoic acid in ApcMin/+ mice. J Nutr 130: 1153–1158.

Pozzi A, Yan X, Macias-Perez I, Wei S, Hata AN, Breyer RM *et al.* (2004). Colon carcinoma cell growth is associated with prostaglandin E2/EP4 receptor-evoked ERK activation. J Biol Chem 279: 29797–29804.

Rao R, Redha R, Macias-Perez I, Su Y, Hao C, Zent R *et al.* (2007). Prostaglandin E2-EP4 receptor promotes endothelial cell migration via ERK activation and angiogenesis in vivo. J Biol Chem 282: 16959–16968.

Togni V, Ota CCC, Folador A, Júnior OT, Aikawa J, Yamazaki RK *et al.* (2003). Cancer cachexia and tumor growth reduction in Walker 256 tumor-bearing rats supplemented with N-3 polyunsaturated fatty acids for one generation. Nutr Cancer 46: 52–58.

Vanamala J, Glagolenko A, Yang P, Carroll RJ, Murphy ME, Newman RA *et al.* (2008). Dietary fish oil and pectin enhance colonocyte apoptosis in part through suppression of PPARδ/PGE2 and elevation of PGE3. Carcinogenesis 29: 790–796.

Wang D, DuBois RN (2010). The role of COX-2 in intestinal inflammation and colorectal cancer. Oncogene 29: 781–788.

West NJ, Clark SK, Phillips RKS, Hutchinson JM, Leicester RJ, Belluzzi A *et al.* (2010). Eicosapentaenoic acid reduces rectal polyp number and size in familial adenomatous polyposis. Gut 59: 918–925.

Yang P, Chan D, Felix E, Cartwright C, Menter DG, Madden T *et al.* (2004). Formation and antiproliferative effect of prostaglandin E3 from eicosapentaenoic acid in human lung cancer cells. J Lipid Res 45: 1030–1039.

Zhong YS, Lu SX, Xu JM (2008). Tumor proliferation and apoptosis after preoperative hepatic regional arterial infusion chemotherapy in prevention of liver metastasis after colorectal cancer surgery. Zhonghua Wai Ke Za Zhi 46: 1229–1233.

Supporting information

Additional Supporting Information may be found in the online version of this article:

Figure S1 (A) Daily food intake per cage before and after intrasplenic injection. Data are presented as the mean intake

of chow in g from two cages per treatment group. Alternate day values are presented to aid visualization. There was no significant difference between food intakes among the treatment groups. Repeated measures ANOVA $F = 9.8$, $P = 0.09$. (B) Body weight presented as the mean and SEM of individual body weights in the three treatment groups on alternate days. There was no significant difference in body weight at killing (day 28) between the control and 5% EPA-FFA-treated groups ($P = 0.15$; one-way ANOVA with *post hoc* Bonferroni analysis).

Figure S2 Fatty liver in *BALB/C AnN* mice. Microvesicular steatosis was evident in hepatocytes neighbouring tumour tissue (asterisk) in H&E-stained fixed liver sections from all animals. The example has a steatosis score of 3. Oil Red O staining of frozen tissue confirmed excess fat content in hepatocytes (stained red). Assessment of the degree of steatosis in H&E-stained sections by two observers, who were blinded to the treatment allocation of each section, did not reveal any significant difference between the treatment groups.

Figure S3 Immunohistochemistry for Cox-2 in MC-26 mouse CRC cell tumours. Staining of MC-26 cells was not uniform in metastatic tumours. Strongly Cox-2-expressing cells (often with prominent peri-nuclear staining) were present throughout tumours, often surrounded by weakly-staining or negative cells. Examples of Cox-2 immunoreactivity scoring of tumour tissue. (A) score 0; (B) score 1; (C) score 3; (D) score 6. Size bar = 100 µm in all cases.

Figure S4 Individual EPA/AA ratios, E-type PG levels and biomarkers of tumour growth in mice from all three treatment groups. The Spearman correlation coefficient and *P* value for the relationship is noted above each dot-plot.

Figure S5 MTT assay of MC-26 mouse CRC cell viability in the presence of EPA-FFA for 24 h. Data are expressed as the mean ± SD of the percentage cell viability compared with control for three independent experiments. $IC_{50} = 236 \pm 26$ mM.

Table S1 Composition of the test diets (%)

Please note: Wiley-Blackwell are not responsible for the content or functionality of any supporting materials supplied by the authors. Any queries (other than missing material) should be directed to the corresponding author for the article.